文章编号：1007 - 1482(2005)03 - 0176 - 06 ·论著·

Navigation path acquisition in virtual endoscopy

Jianfei LIU[1,2], Xiaopeng ZHANG[1,2]

(1. Sino-French Laboratory LIAMA, Institute of Automation, CAS, Beijing 100080, China;
2. National Laboratory of Pattern Recognition, Institute of Automation, CAS, Beijing100080, China)

Abstract: Navigation path planning and collision detection are difficult problems in virtual navigation in complex environments, especially in simulated endoscopic navigation inside human organs. We solve these problems through a combination of shape keeping skeleton and the distance from each internal point to boundary. Combining distance transform and topological thinning, Distance Contained Centerline (DCC) algorithm is presented to extract a line-shaped skeleton of an elongated volume and compute the distance from centerline to each erosion layer. Spurious branches of a skeleton are adaptively removed through the distance threshold and the branch length threshold. In addition, we use line-simulation to smooth the skeleton. Experiments show that the skeleton obtained through DCC represents the complex shape of elongated objects well and it is useful for guiding virtual navigation.

Key words: 3D thinning; distance transform; virtual endoscopy; path extraction

虚拟内窥镜中漫游路径的获取*

刘剑飞[1,2], 张晓鹏[1,2]

(1. 中国科学院自动化研究所中法联合实验室, 北京 100080;
2. 中国科学院自动化研究所模式识别国家重点实验室, 北京 100080)

摘 要：漫游路径提取和碰撞检测是复杂环境下虚拟漫游的两个重要难题,尤其在人体器官中的虚拟内窥漫游。我们通过结合保持物体形状的骨架和内部点到边界的距离解决了上述两个难题。综合了距离变换和拓补细化,本文提出了包含距离信息的中心线提取算法。该算法可以有效的提取出管状物体的单体素连接的中心线并能记录中心线到删除层的距离。骨架上的杂枝也可通过距离阈值和长度阈值予以删除。此外,我们还结合了直线模拟来光滑骨架。实验结果表面该算法得到的骨架能够很好地表示复杂的管状物体并能有效的指导漫游。

关键词：三维细化；距离变换；虚拟内窥镜；路径提取
中图分类号：TP391.41 **文献标识码**：A

In recent years, Virtual endoscopy (VE) has been widely employed to examine the interior structures of human organs[1~4]. Incorporating the technologies of medical imaging and computer graphics, VE becomes a promising alternative tool to conventional endoscopy (CE). Compared with CE, VE is noninvasive, cost-effective, free of risks, and capable of viewing some locations and directions in which CE may have limited views.

A crucial component of VE is to carefully design a centerline to view the entire lumen for complex geometrical organs, such as the airway, the pulmonary tree,

收稿日期：2005 - 08 - 26
通讯作者：张晓鹏,副研究员, E-mail：xpzhany@ nlpr. ia. ac. cn

and the colon. Skeletonization provides an effective method to extract a thinner centerline while highlighting structural features. Skeleton not only provides accurate geometric measurement, but also supports automatic path planning for both planned and interactive navigations. The desired skeleton should preserve connectivity, hold centricity, keep topology, be insensitive to boundary noise, be refined by parameters, and be effective for collision detection.

Based on these requirements, many methods have been studied for 3D skeletonization or centerline extraction of volumetric objects. Most of them can be divided into three classes: manual extraction[5], topological thinning[6~9], and distance transform[10~17].

The essential idea of manual extraction is to label the center of objects on each image slice by hand and then to connect these marked points. It is time-intensive and the result is in no case more accurate than those of other methods.

Topological thinning is one way of skeletonization, which yields the most accurate result. It iteratively erodes a volumetric object layer by layer until only one central layer, the skeleton, is left. However, the repetitive procedure is quite time-consuming, especially for identifying the "simple point". Ma and Sonka[6] proposed a fully parallel, connectivity-preserving, 3D thinning algorithm to reduce computational expenses. It avoids expensive testing of "simple point" by comparing 26-neighborhood of the points with specific templates. But this algorithm often generates a skeleton with many spurious branches and leaves unorganized discrete points.

The most popular technique, distance transform, is considered as the fastest one among the three classes. It tries to extract skeletal points directly by testing points' neighborhood based on a distance transform, which is an approximation of the Euclidean distance. It usually takes three steps: 1) perform distance transform from seed points to each voxel inside the 3D object, 2) detect all local maxima in terms of distance value, 3) extract the shortest path from all local maxima to the source point by the steepest backtracing. Although this method can improve computational efficiency, the result may hug the corners rather than follow the medial axis around sharp turns. Wan[13] presented an efficient algorithm based on the exact Euclidean distance to solve the hugging problem, but it is not very efficient in preserving topology, especially for elongated objects with complex geometry.

There are also other varieties of path extraction and skeleton methods proposed[18~20]. They tried to extract skeleton from 3D Scattered Data. However, most of them can't solve irregular medical images, especially for extracting a smooth centerline to guide navigation.

In this paper, a novel skeletonization algorithm, Distance Contained Centerline (DCC) algorithm, has been proposed to overcome the limitations of the previous methods and satisfy six requirements described above. It also computes the distance between each internal point and object boundary to solve the problem of viewpoint collision in VE. Furthermore, it integrates voxel-coding to reorganize skeleton and prune spurious branches.

The remainder of this paper is as follows. Section 2 reviews template based topological thinning and voxel-coding techniques. DCC is described in section 3, consisting of data preprocessing, distance contained parallel thinning, topology reorganization, and centerline smoothing. Experimental results will be analyzed in section 4. Finally, conclusions are presented in section 5.

1. Related Work

The basis of template based thinning and voxel-coding is digital topology. Therefore, the conceptions for it are covered here[6,21,22].

1.1 Template Based Thinning

In Ma's topological thinning algorithm, specific templates are designed to extract the skeleton. These templates can be obtained by rotations and reflections of 4 so-called template cores (A, B, C, D) shown in figure 2. In template cores, the white point is a background point, the black point is an object point, and the unmarked point is a "do not care" point that can represent either a background point or an object point.

For the D core template, p must be a simple point.

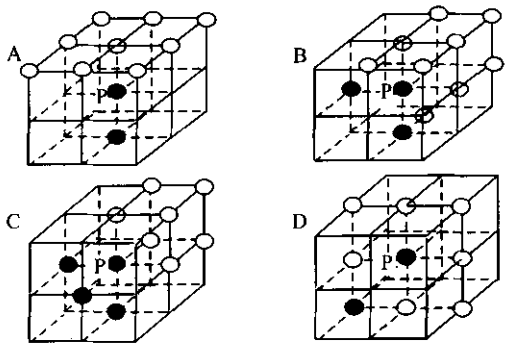

Fig. 1 Four template cores.

However, checking the 26-neighborhood is not adequate to keep connectivity, and several templates must check extra points in an extended neighborhood. In figure 3, two templates of core D and the extra tests in these templates are illustrated, where at least one point at the place of white squares is an object point. In implementation, when the neighborhood configuration of an object point in a 3D image satisfies any deleting template, the point is optional to be deleted. And owing to the parallel nature of the algorithm, a set of object points can be deleted in each iterative step.

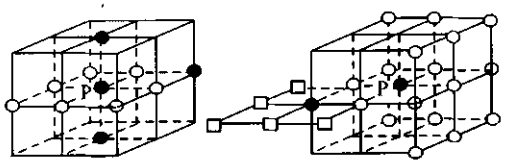

Fig. 2 Two kinds of templates obtained from core D.

1.2 Voxel-coding

Voxel-coding is a kind of distance transform providing an approximation to the minimum Euclidean distance of object voxels from boundary or background voxels. It begins with a set of seed voxels S, follows a specific coding scheme or metric M within a volumetric object R, and iteratively assigns the value voxel-by-voxel until constraint conditions are met.

In order to simplify the complexity, coding metric adopts integer values to approximate the local distance for moving to a 6-, 18-, or 26-neighbor. For example, optimal integers 3, 4, 5 can be used, and is denoted as《3, 4, 5》. Often,《1, 2, 3》and《3, 4, 5》metrics are applied[17]. Boundary voxels or a single reference voxel are often chosen as a seed set, which are called BS-Coding or SS-Coding respectively.

An important application of voxel-coding is shortest path extraction (SPE). The problem is how to extract the shortest path between two object points, *source* and *destination*, in a volumetric object R. First, *source* is set as a seed point and a special coding metric is used to propagate until *destination* is reached. Second, *destination* is taken as the first point of the path and the next path point is the minimal value in the 26 neighborhood of the *destination*, recursively until the last point is met. The last point must be *source* because it has the smallest code in the field.

2. Distance Contained Centerline

DCC can be categorized as a path planning method in which the path is first initialized and centralized by parallel thinning. Then voxel-coding is applied to refine and reorganize it. DCC consists of the following steps: data pre-processing, distance contained parallel thinning, topology reorganization, and centerline smoothing.

2.1 Distance Contained Parallel Thinning

In DCC, an initial skeleton is similar to template based thinning. However, we make some modifications in its application, which is summarized in figure 5.

Due to the extensive computations of simple point test in core D deleting templates, DCC implements them separately and omits "simple point" test in them. However, when a point satisfying Core D templates is deleted in parallel with its 26-neighbor points, it is necessary to demonstrate that sequential deleting is equal to parallel deleting and so for the simple point test.

There are three reasons to prove the effectiveness of our change. First, we observe that the object point p is just a simple point. In figure 3, $T_{26}(p, V) = 1$ and

① Although these properties have held for the numerous experiments we have performed, we unfortunately do not have formal proofs for them as yet

$T_6(p,\bar{V}=1)$ can be found in p 's 26-neighborhood, so p is a simple point according to definition 1. Although other core D templates can be obtained through reflections and rotations, reflection and rotation don 't change the topology of p 's 26-neighborhood. Therefore, all core D 's templates can delete points in parallel regardless of whether p is a simple point and this change doesn 't violate Ma 's mathematical verification of the connectivity preservation. Second, just as the demonstration in[1], performing these templates in a separate iteration can guarantee the equivalence between sequential thinning and parallel thinning. Third, core D 's templates are seldom used because some object points in core D are 18-connected to p. Therefore, the separate iteration doesn 't influence the parallelism much.

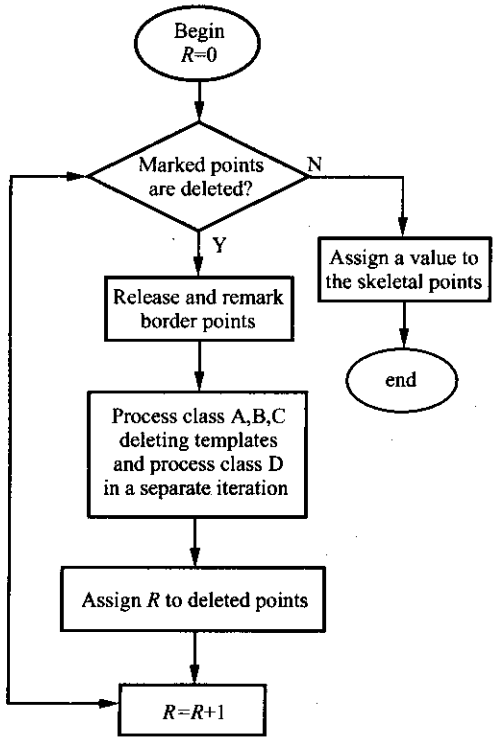

Fig. 3 Flowchart of parallel thinning.

Another improvement is to evaluate a distance from boundary for every internal point when performing 3D parallel thinning. The idea is that the process of thinning erodes an object layer by layer until only the centralized path is left. Hence, in each step of erosion, only border points are processed and the step is deemed as the distance from boundary to the current point. This distance is conservative① and useful for collision detection. When implementing parallel thinning, all border points are first marked in each iterative step and this step is repeated until no marked point can be deleted. If these marked points are deleted in this step, they are assigned a natural number representing the distance from boundary to them. The thinning process stops when skeletal points are reached. Then the value of each skeletal point is given by its 26-neighbor 's minimum value plus 1. Part of the result in one slice of the 3D image is shown in figure 6, where gray squares denote background voxels and white squares represent object voxels. The number in black is the distance value between the internal voxel and the boundary, and the number in red is the distance of skeleton voxel to the boundary.

2.2 Topology reorganization

After thinning, the initial skeleton S can be obtained, which is composed by the skeleton voxel in figure 6. Due to the irregularity of real objects, S commonly has many spurious branches such as blue squares shown in figure 6. Besides this drawback, the skeleton only keeps position information, but doesn 't provide any topology knowledge. Spurious branches must be pruned and the skeleton should be reorganized for intuitive navigation in VE. However, there is little work on these aspects in literature. DCC combines voxel-coding to solve the above problems successfully. The pseudeocode is summarized in figure 7.

Step 1：Since S is simpler than a 3D digital image, SS-coding is just used within S. In SS-coding, considerable attention should be paid to the selection of seed points because the choice of them plays a fundamental role in the results of topology reorganization. Usually, end-points can be selected as seed points. An object point is called an end point if there is only one object point in its 26-neighborhood. Otherwise, the middle point of a connected region in the first slice can be chosen as a seed point. We use《3-4-5》as coding metric because the exact value of S needs to be known.

Step 2：In DCC, an object point is called a local maximal point if its distance value is larger than all object points in its 26-neighborhood. It is called merging

point if at least two object points in its 26-neigborhood have smaller distance values and at least two of them are not 26-connected. Following the above definitions, two arrays, LMArray and HMArray, can be established on S. LMArray stores local maximal points in descending order and HMArray stores unconnected object points in the 26-neighbor of the merging points.

Step 3: Branches in the final skeleton can be extracted beginning with LMArray 's every point by SPE. An array, BranchArray, stores its points and an array, LabelArray, stores BranchArray of each processed branch. SPE is terminated if the extracted point is the seed point or the point of another branch. If the point of another branch is met, the label of this branch is inserted at the beginning of the BranchArray as a mark for parent branch. If a seed point is reached, a special value is inserted at the initial position of the BranchArray.

Step 4: In order to deal with object holes, the points, absent from the BranchArray of the extracted branches while in HMArray, are selected as starting points to extract other unprocessed branches by SPE.

Step 5: In DCC, two thresholds, distance threshold and length threshold, are adjusted to refine the final skeleton, which not only can remove the spurious branches adaptively, but also can control the choice of the trunk precisely. A BranchArray is removed if the number of its points is below length threshold, or the average distance of this branch is below distance threshold, and it has no child branch. Then all branches are relabeled and parent-child relationships are updated. This process is repeated until no branch can be deleted. Ultimately we reorganize the skeleton and obtain a thin connected skeleton.

3. Experiments and Applications

DCC is tested on two kinds of dataset: 3D tree models which are obtained through filling the volume of polygon tree models generated by commercial software AMAPTM, and medical models obtained from CT images. We use tree models to test our algorithm because they are also complex elongated objects. These datasets have been implemented in Visual C + + and run on a Pentium IV PC with 2.4G CPU and 512M RAM. Experiment details are listed in table 1.

Tab. 1 Experiment details

Data / Model	Voxel number of dataset	Voxel number of skeleton	Number of branch	Implementation time (second)
Willow tree model	84736	8683	185	885.33
Holly tree model	23855	2134	58	45.03
Airway model	164111	716	12	132.23
Colon model	317124	183	1	245.55

Figure 8 shows the comparison between Ma 's results and DCC 's results, where original objects are shown in the left volume, Ma 's results are illustrated in the center volume, and DCC 's results are listed in the right volume. They all keep the connectivity, but DCC 's results are more singular than Ma 's results in red square. In the top two rows, Ma 's results contain many spurious branches in red circle, but there are few spurious branches in the bottom two rows. We consider it is because tree models are more regular than medical objects. But all spurious branches can be pruned in our results.

By adjusting length threshold and distance threshold, different results can be achieved in figure 9. Length threshold is applied in the top row. It is 20 in the left volume, center 35, and right 50. In the bottom row, distance threshold is used, left 1, center 2, and right 3. These thresholds can locate main characters of the object quickly and are fairly convenient to select different path of viewpoint in navigation.

Overlaying DCC 's results over the objects are illustrated in figure 10, where the object is in white and the skeleton is in red. It not only shows that the skeleton generated by DCC is smooth and singular, but also demonstrates that the skeleton keeps the object topology and follows the medial axis around sharp turns. Therefore, DCC combines advantages of distance transform and topological thinning.

Two scenes in virtual navigation guided by DCC 's result are illustrated in figure 11. The figure on the left displays navigation result in airway bifurcation. The one on the right displays the result in the colon. They demonstrate the effectiveness of DCC based virtual nav-

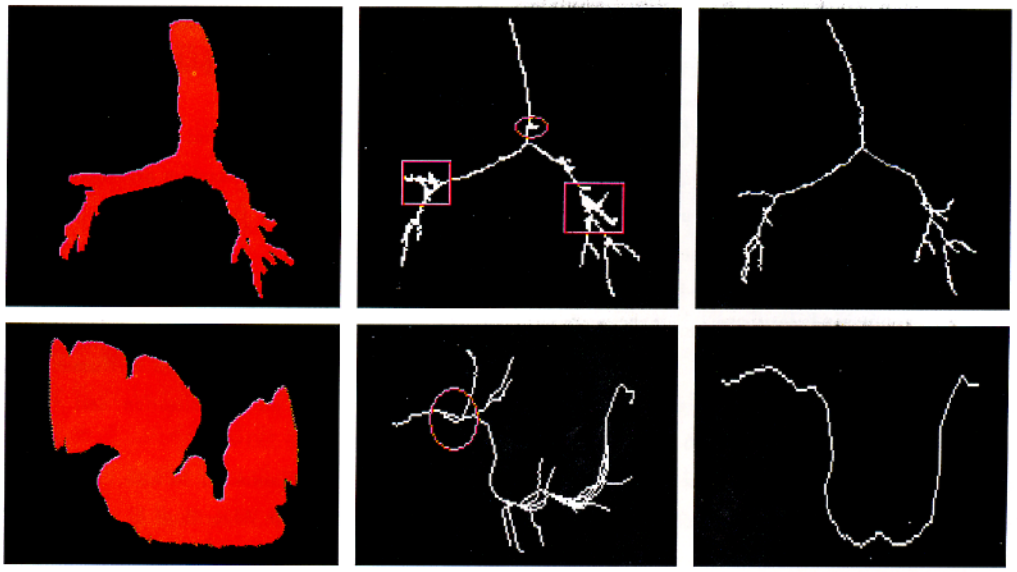

Fig. 4 Comparison between Ma 's resusts and DCC 's results.

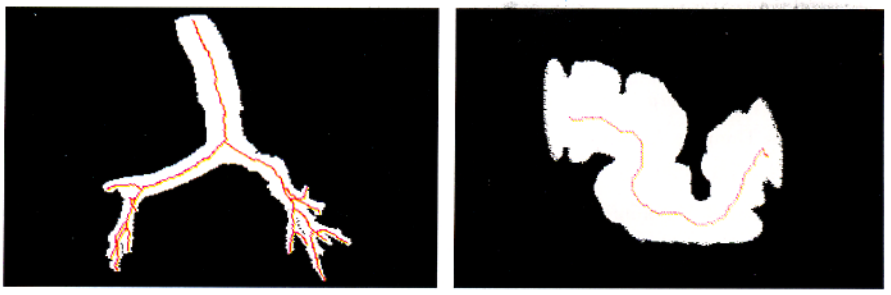

Fig. 5 Overlaying centerline over their 3D models.

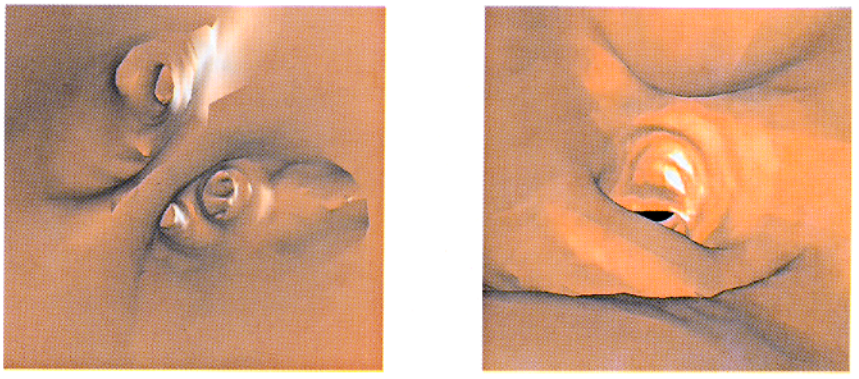

Fig. 6 Guided virtual navigation in human trachea.

igation in human organs and avoid viewpoint collision.

4. Conclusions and Future Work

From the above descriptions and experiments, it is evident that DCC algorithm mentioned in this paper has four advantages for centerline extraction：1) keeping the object topology well, 2) being centered with respect to object boundary, 3) getting the smooth and refined skeleton, 4) being effective for collision detection.

References：

[1] Anna Vilanova, Andreas König and Eduard Gröller. VirEn：A Virtual Endoscopy System [J]. MACHINES GRAPHICS and VISION, 1999, 8(3)：469 – 487.

[2] K Mori, Y Suenaga, J ToriWaki, J Hasegawa, H Anno, K Katada and H Natori. Automated display of anatomical name of branchial branches in virtual bronchoscopy system and its application as a training tool for medical students[J]. Proceedings of SPIE, 1999,3660:301 - 312.

[3] L Hong, S Muraki, A Kaufman, D Bartz and T He. Virtual voyage: Interactive navigation in the human colon [C]. Proc SIGGRAPH '97,1997. 27 - 34.

[4] R Yagel, D Stredney, G J Wiet, P Schmalbrock, L Rosenberg, D J Sessanna and Y Kurzion. Building a virtual environment for endoscopic sinus surgery simulation [J]. Computers and Graphics,1996,20(6):813 - 823.

[5] Y Ge, D Stelts and D Vining. 3D skeleton for virtual colonoscopy[C]. proc 4th Int conf Visualization in Biomedical Computing (Lecture Notes in Computer Science 0302-9743m),1999. 449 - 454.

[6] C Min Ma and M Sonka. A fully parallel 3D thinning algorithm and its application[J]. Computer Vision and Image Understanding, 1996, 64(3):420 - 433.

[7] J Mukerjee, P P Das and B N Chatterji. Thinning of 3D images using the Safe Point Thinning Algorithm (SPTA) [J]. Pattern Recognition Letters,1989,10:167 - 173.

[8] Y F Tsao and K S Fu. A Parallel Thinning Algorithm for 3D Pictures[J]. Computer Graphics and Image Processing,1981,17:315 - 331.

[9] T Pavlidis. A Thinning Algorithm for Discrete Binary Images [J]. Computer Graphics and Image Processing, 1980,13:142 - 157.

[10] Y Zhou and A Toga. Efficient skeletonization of volumetric objects[J]. IEEE Trans Vis Comput Graph,1999,5: 196 - 209.

[11] I Bitter, M sato, M Bender, K McDonnel, A Kaufman, and M Wan. CEASAR: A smooth, accurate and robust centerline-extraction algorithm [C]. Proc Viualization 2000, 2000:45 - 52.

[12] M Sato, I Bitter, M Bender, A Kaufman, and M Nakajima. TEASAR: Tree-structure extraction algorithm for accurate and robust skeletons[C]. Proc 8th Pacific Conf. Computer Graphics and Applications,2000. 281 - 289.

[13] M Wan, Z Liang, Qi Ke, L Hong, I Bitter and A Kaufman. Automatic Centerline Extraction for Virtual Colonoscopy[J]. IEEE Trans Med Imag, 2002, 21 (12).

[14] Ali Shanhrokni, Hamid Soltanian-Zadeh and Reza A Zoroofi. Fast skeletonization algorithm for 3D elongated objects[C]. San Diego: Proc of SPIE Medical Imaging 2001,2001.

[15] Taosong He, Lichan Hong, Dongqing Chen, and Zhengrong Liang. Reliable Path for Virtual Endoscopy: Ensuring Complete Examination of Human Organs[J]. IEEE Transactions on Visualization and Computer Graphics, 2001,7(4):333 - 341.

[16] I Bitter, A Kaufman, M sato. Penalized-Distance Volumetric Skeleton Algorithm[J]. IEEE Transactions on Visualization and Computer Graphics, 2001,7(3):195 - 206.

[17] G Borgefors. Distance Transformations on Digital Images [J]. Computer Vision, Graphics, and Image Processing, 1986,34:344 - 371.

[18] A Verroust and F Lazarus. Extracting Skeletal Curves from 3D Scattered Data[C]. Rapport de Recherche INRIA no 3250, 1997.

[19] A Verroust and F Lazarus. Extracting Skeletal Curves from 3D Scattered Data[C]. Aizu, Japan: Shape Modeling International '99, 1999.

[20] A Verroust and F Lazarus. Extracting Skeletal Curves from 3D Scattered Data [J]. The Visual Computer, 2000,16(1):15 - 25.

[21] T Y Kong and A Rosenfeld. Digital Topology: introduction and survey[J]. Computer Vision, Graphics and Image Processing,1989,48:357 - 393.

[22] G Betrand and G Malandain. A new characterization of three dimensional simple points[J]. Pattern Recognition Letters,1994,15:169 - 175.